

# Directed Metalation Cascade To Access Highly Functionalized Thieno[2,3-*f*]benzofuran and Exploration as Building Blocks for Organic Electronics

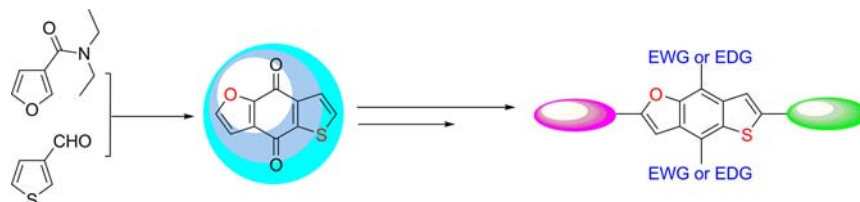
Yves Aeschi,<sup>†,§</sup> Hui Li,<sup>†,§</sup> Zhencai Cao,<sup>‡</sup> Songjie Chen,<sup>†</sup> Anneliese Amacher,<sup>†</sup> Nathalie Bieri,<sup>†</sup>  
Bilal Özen,<sup>†</sup> Juerg Hauser,<sup>†</sup> Silvio Decurtins,<sup>†</sup> Songting Tan,<sup>‡</sup> and Shi-Xia Liu<sup>\*,†</sup>

Departement für Chemie und Biochemie, Universität Bern, Freiestrasse 3,  
CH-3012 Bern, Switzerland, and College of Chemistry, Xiangtan University,  
Xiangtan 411105, P.R. China

liu@iac.unibe.ch

Received September 26, 2013

## ABSTRACT



A tandem directed metalation has been successfully applied to the preparation of thieno[2,3-*f*]benzofuran-4,8-dione, providing an efficient and facile approach to symmetrically and unsymmetrically functionalize the thieno[2,3-*f*]benzofuran core at the 2,6 positions as well as to introduce the electron-withdrawing or -donating groups (EWG or EDG) at its 4,8 positions. The presence of various functional groups makes late-stage derivatization attainable.

Benzodichalcogenophene (BDC) derivatives, in particular benzodifuran (BDF) and benzodithiophene (BDT), are of prime interest as organic semiconductors due to their fascinating features including structural symmetry and planarity as well as rigid and  $\pi$ -extended conjugation which can enhance electron delocalization and intermolecular interactions to improve charge mobility.<sup>1–6</sup> They are most commonly used as  $\pi$ -electron donors for high-performance organic electronics, such as bulk heterojunction (BHJ) and dye-sensitized solar cells (DSSC), organic

field effect transistors (OFET), and organic light-emitting diodes (OLED).<sup>7–15</sup> For example, BDT-based small-molecule BHJ solar cells show the hitherto reported highest efficiency of 7.4%.<sup>8</sup> The single micrometer ribbon

(7) Chen, H.-Y.; Hou, J.; Zhang, S.; Liang, Y.; Yang, G.; Yang, Y.; Yu, L.; Wu, Y.; Li, G. *Nat. Photon.* **2009**, *3*, 649–653.

(8) Zhou, J.; Wan, X.; Liu, Y.; Zuo, Y.; Li, Z.; He, G.; Long, G.; Ni, W.; Li, C.; Su, X.; Chen, Y. *J. Am. Chem. Soc.* **2012**, *134*, 16345–16351.

(9) Yi, C.; Blum, C.; Lehmann, M.; Keller, S.; Liu, S.-X.; Frei, G.; Neels, A.; Hauser, J.; Schürch, S.; Decurtins, S. *J. Org. Chem.* **2010**, *75*, 3350–3357.

(10) Keller, S.; Yi, C.; Li, C.; Liu, S.-X.; Blum, C.; Frei, G.; Sereda, O.; Neels, A.; Wandlowski, T.; Decurtins, S. *Org. Biomol. Chem.* **2011**, *9*, 6410–6416.

(11) Li, H.; Jiang, P.; Yi, C.; Li, C.; Liu, S.-X.; Tan, S.; Zhao, B.; Braun, J.; Meier, W.; Wandlowski, T.; Decurtins, S. *Macromolecules* **2010**, *43*, 8058–8062.

(12) Li, H.; Tang, P.; Zhao, Y.; Liu, S.-X.; Aeschi, Y.; Deng, L.; Braun, J.; Zhao, B.; Liu, Y.; Tan, S.; Meier, W.; Decurtins, S. *J. Polym. Sci., Part A: Polym. Chem.* **2012**, *50*, 2935–2943.

(13) Huo, L.; Ye, L.; Wu, Y.; Li, Z.; Guo, X.; Zhang, M.; Zhang, S.; Hou, J. *Macromolecules* **2012**, *45*, 6923–6929.

(14) Didane, Y.; Mehl, G. H.; Kumagai, A.; Yoshimoto, N.; Vidolot-Ackermann, C.; Brisset, H. *J. Am. Chem. Soc.* **2008**, *130*, 17681–17683.

(15) Wang, S.; Ren, S.; Xiong, Y.; Wang, M.; Gao, X.; Li, H. *ACS Appl. Mater. Interfaces* **2012**, *5*, 663–671.

<sup>†</sup> Universität Bern.

<sup>‡</sup> Xiangtan University.

<sup>§</sup> These authors contributed equally to this work.

(1) Zhou, H.; Yang, L.; Stuart, A. C.; Price, S. C.; Liu, S.; You, W. *Angew. Chem., Int. Ed.* **2011**, *50*, 2995–2998.

(2) Wang, C.; Zhao, B.; Cao, Z.; Shen, P.; Tan, Z.; Li, X.; Tan, S. *Chem. Commun.* **2013**, *49*, 3857–3859.

(3) Gu, Z.; Shen, P.; Tsang, S.-W.; Tao, Y.; Zhao, B.; Tang, P.; Nie, Y.; Fang, Y.; Tan, S. *Chem. Commun.* **2011**, *47*, 9381–9383.

(4) Tsuji, H.; Mitsui, C.; Ilies, L.; Sato, Y.; Nakamura, E. *J. Am. Chem. Soc.* **2007**, *129*, 11902–11903.

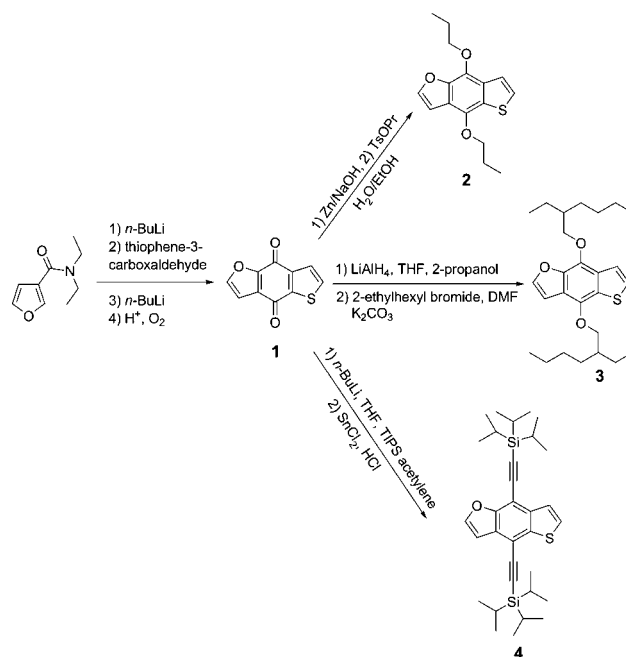
(5) Tsuji, H.; Mitsui, C.; Sato, Y.; Nakamura, E. *Adv. Mater.* **2009**, *21*, 3776–3779.

(6) Anthony, J. E. *Chem. Rev.* **2006**, *106*, 5028–5048.

transistor of a BDT derivative displayed high mobility up to  $0.81 \text{ cm}^2 \text{ V}^{-1} \text{ s}^{-1}$ .<sup>15</sup> Since we developed a facile and efficient synthetic route to fully functionalized BDF derivatives,<sup>9,10</sup> which allowed us to further prepare the first BDF-based copolymers for BHJ solar cells,<sup>11,12</sup> an increasing number of BDF-based polymers and small conjugated molecules has appeared in the literature, with a high efficiency up to 6.3%.<sup>13</sup> In contrast to an extensive investigation on BDT, thieno[2,3-*f*]benzofuran (TBF), as a structural hybrid of BDF and BDT, has not yet been explored, owing to the limited preparative accessibility and the lack of an efficient and convenient synthetic methodology. To date, despite successful and well-established synthetic approaches to the BDF and BDT derivatives,<sup>9–17</sup> there has been only one report on the synthesis of the key precursor thieno[2,3-*f*]benzofuran-4,8-dione (**1**, Scheme 1) with a poor yield of 24% under strict reaction conditions.<sup>18</sup> Our keen interest in TBF-based chromophores stems from the assumption that they show remarkably different optoelectronic properties from BDF and BDT derivatives by replacement of a thiophene ring with a furan in the BDT core, as reported in the case of thieno[2,3-*b*]thiophene.<sup>19</sup> Finally, a synergetic effect of thiophene and furan rings in the TBF molecules on device performance is of great importance. As a consequence, we have optimized the synthetic procedure to produce **1** with a marked improvement of the reported yield, whereby various TBF-based building blocks bearing different functional groups such as Br, I and boronic ester can readily be prepared for late-stage derivatization via Suzuki, Sonogashira, and Stille coupling reactions. As an example, a series of TBF-based donor–acceptor alternating polymers have been synthesized, fully characterized, and tested as BHJ solar cell devices.

As illustrated in Scheme 1, the key precursor **1** was obtained by the condensation of thiophene-3-carboxaldehyde with lithiated furan precursor. Lithiation with *n*-BuLi instead of *s*-BuLi/TMEDA within a well-adjusted reaction time turns out to be more efficient due to the elimination of side reactions. Therefore, synthesis of **1** was accomplished under a much milder reaction condition with a much higher yield of 60% compared to the literature.<sup>18</sup> Compounds **2–4** were prepared to probe the electronic effects engendered by the addition of electron-donating (alkoxy) or electron-withdrawing (triisopropylsilyl (TIPS)ethynyl) groups to the 4,8-positions of the redox-active TBF chromophore. Reduction of **1** and subsequent alkylation afforded **2** and **3** in 51% and 72% yields, respectively. Compound **4** was readily prepared in 60% yield via a nucleophilic attack on **1** with a resulting

**Scheme 1.** Synthetic Route to TBF Derivatives **1–4**



TIPS-acetylide followed by the subsequent deoxygenation and aromatization with hydrochloric acid  $\text{SnCl}_2$  solution. Moreover, the corresponding BDF and BDT analogues (**I–IV**, Figure 1) were synthesized according to similar procedures, allowing a comparative study of their electrochemical and photophysical properties.

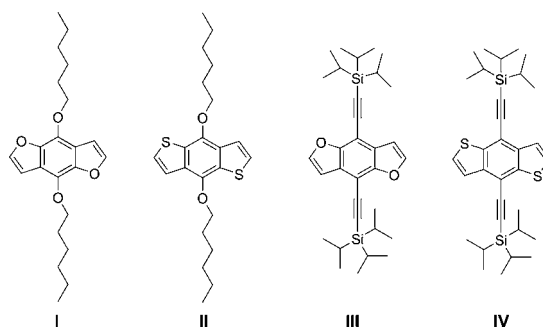


**Figure 1.** Chemical structures of BDF and BDT analogues **I–IV**.

Due to the inherent asymmetry of TBF derivatives, a regioselective nucleophilic bromination of **2** can be accomplished via a lithiation followed by the addition of  $\text{CBr}_4$ , leading to the formation of two regioisomers **5** and **6** with a molar ratio of 6:4 in total yield of 70% (Scheme 2). They can be isolated simply by chromatography. A Vilsmeier reaction has been further applied to introduce a functional aldehyde group, thus yielding unsymmetrically functionalized TBF derivatives **7** and **8** in good yields.

Further functionalization of **3** has been conducted through the introduction of Br, I and boronic ester groups,

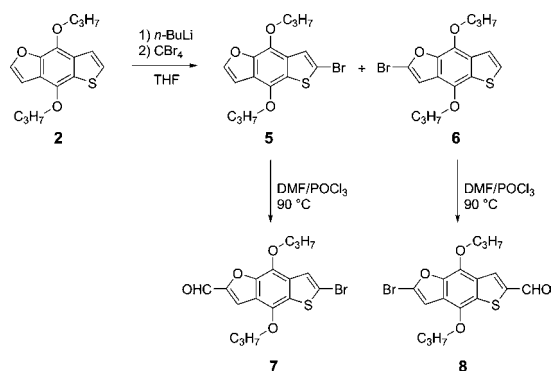
(16) (a) Abdul-Aziz, M.; Auping, J. V.; Meador, M. A. *J. Org. Chem.* **1995**, *60*, 1303–1308. (b) Hosseiny Davarani, S. S.; Fakhari, A. R.; Fumani, N. S.; Kalate-bojdi, M. *Electrochem. Commun.* **2008**, *10*, 1765–1768. (c) Hou, J.; Park, M.-H.; Zhang, S.; Yao, Y.; Chen, L.-M.; Li, J.-H.; Yang, Y. *Macromolecules* **2008**, *41*, 6012–6018. (d) Beimling, P.; Kossmehl, G. *Chem. Ber* **1986**, *119*, 3198–3203.

(17) Takimiya, K.; Konda, Y.; Ebata, H.; Niihara, N.; Otsubo, T. *J. Org. Chem.* **2005**, *70*, 10569–10571.

(18) Watanabe, M.; Snieckus, V. *J. Am. Chem. Soc.* **1980**, *102*, 1457–1460.

(19) Henssler, J. T.; Matzger, A. *J. Org. Lett.* **2009**, *11*, 3144–3147.

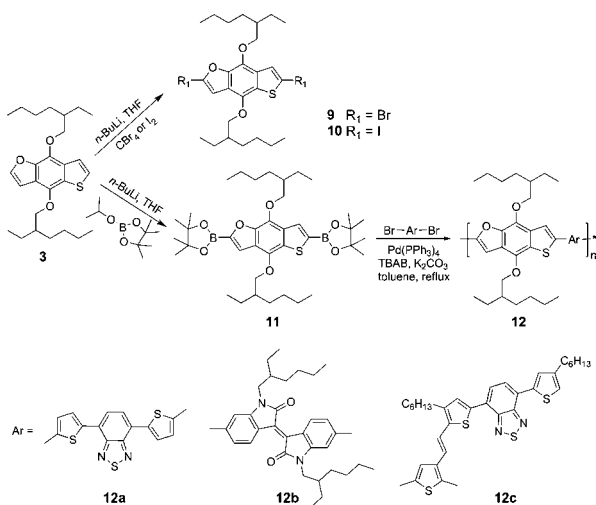
**Scheme 2.** Synthetic Route to Unsymmetrically Functionalized TBF Derivatives **5–8**



as shown in Scheme 3. Bromination/iodination via double deprotonation in the presence of *n*-BuLi followed by treatment with CBr<sub>4</sub> or elemental iodine gave the corresponding products **9** and **10** in yields of 70% and 30%. Similarly, the precursor **11** for the polymers was obtained in 54% yield by double deprotonation of **3** and subsequent nucleophilic attack on 4,4,5,5-tetramethyl-2-isopropoxy-1,3,2-dioxaborolane. Three alternating D–A copolymers were synthesized via Suzuki coupling of **11** with different acceptors (isoindigo, 4,7-dithienylbenzothiadiazole or 3-vinylthienyldithienylbenzothiadiazole).

All these new TBF derivatives have been fully characterized; a single-crystal structure has been resolved in the case of **4** (Supporting Information).

**Scheme 3.** Synthetic Route to Symmetrically Functionalized TBF Derivatives **9–11** as Well as Polymers **12a–c**



The photophysical properties of TBF derivatives **3** and **4** along with the analogues **I–IV** were investigated by electronic absorption spectroscopy in dichloromethane (Figure 2, Table 1, and Supporting Information). For the TIPS-ethynyl-substituted BDCs, optical spectra are similar in shape, and all of them strongly absorb up to 400 nm.

The absorption bands show a red-shift in the order of **III**, **4**, and **IV**; in particular, the lower energy transition is shifted significantly more than the higher energy transitions. Also of importance is the increase in intensity of the lower energy band upon moving to heavier chalcogen atoms, possibly indicating increasing charge transfer character. These observations hold true for the alkoxy-substituted BDCs (Supporting Information), indicating that the electronegativity of the heteroatom (O and S) plays a fundamental role in the absorption maxima location.<sup>17,19,20</sup> Introduction of an TIPS-ethynyl substituent instead of alkoxy leads to a significant red-shift (33–41 nm) due to the extension of the conjugated BDC system and the electron withdrawing effect of ethynyl groups. For instance, chromophore **4** displays a lowest energy absorption maximum at 366 nm, which is red-shifted by 34 nm compared to that of **3**. In comparison with the analogous compounds,<sup>9,10,17</sup> the lowest energy absorption band corresponds to the  $\pi$ – $\pi^*$  transition dominated by one electron excitation from HOMO to LUMO. Therefore, the corresponding optical energy gaps are estimated to be in a range from 3.1 to 3.6 eV based on onsets of the lowest energy absorption bands (Table 1).

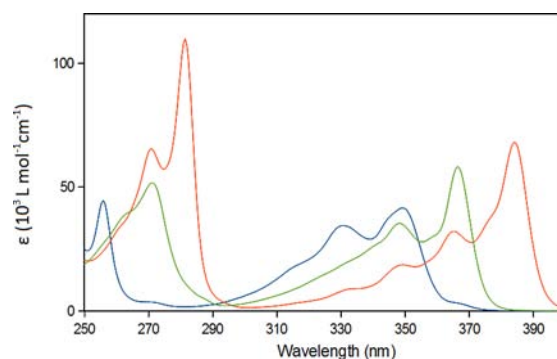


**Figure 2.** Optical spectra of TIPS-ethynyl-substituted BDCs **III** (blue curve), **4** (green curve) and **IV** (red curve) in dichloromethane.

Electrochemical properties of TBF derivatives **3** and **4** as well as the analogues **I–IV** were investigated by cyclic voltammetry (Table 1 and Supporting Information). Both **4** and **III** undergo one irreversible oxidation at 0.97 and 1.06 V respectively, whereas **IV** shows one reversible oxidation at 0.90 V. In contrast, all the alkoxy-substituted BDCs undergo one reversible and one irreversible oxidation. The first oxidation potentials of alkoxy-substituted BDCs are cathodically shifted by at least 0.50 V compared to the corresponding TIPS-ethynyl-substituted BDCs. These results can be attributed to the electron-donating effect of the alkoxy groups on destabilization of the HOMO. In other words, introduction of ethynyl substituents at the 4,8-positions of the BDC core has proven to be

(20) Bryant, J. J.; Lindner, B. D.; Bunz, U. H. *J. Org. Chem.* **2013**, *78*, 1038–1044.

**Table 1.** Lowest Energy Absorption Maxima  $\lambda_{\text{max}}$ , Redox Potentials ( $V$  versus  $\text{Fc}/\text{Fc}^+$ ), HOMO, and LUMO Energy Levels and Optical Band Gaps  $E_{\text{g}}^{\text{opt}}$  of BDC Derivatives

	$\lambda_{\text{max}}^a$ (nm)	$E_{1/2}^{\text{ox1}}$ (V)	$E_{1/2}^{\text{ox2}}$ (V)	$E_{\text{g}}^{\text{opt}}$ (eV)	HOMO <sup>c</sup> (eV)	LUMO <sup>d</sup> (eV)
<b>IV</b>	384	0.90		3.1	−5.58	−2.48
<b>4</b>	366	0.97 <sup>b</sup>		3.3	−5.70	−2.40
<b>III</b>	349	1.06 <sup>b</sup>		3.4	−5.76	−2.36
<b>II</b>	351	0.40	0.86 <sup>b</sup>	3.3	−5.18	−1.88
<b>3</b>	332	0.41	0.95 <sup>b</sup>	3.4	−5.08	−1.68
<b>I</b>	308	0.43	1.00 <sup>b</sup>	3.6	−5.18	−1.58

<sup>a</sup> Measured in  $\text{CH}_2\text{Cl}_2$  solution ( $10^{-5}$  M) with 0.1 M tetra-*n*-butylammonium hexafluorophosphate. <sup>b</sup> Irreversible peaks. <sup>c</sup> Estimated from the onset of oxidation peak. <sup>d</sup> Calculated from the HOMO levels and optical energy band gap, using  $\text{HOMO} + E_{\text{g}}^{\text{opt}}$ .

effective in lowering both LUMO and HOMO energy levels, consistent with the above-mentioned UV–vis spectroscopic results. From the onset of the oxidation peaks, the HOMO levels of these chromophores are roughly estimated under the premise that the energy level of  $\text{Fc}/\text{Fc}^+$  is 4.8 eV below the vacuum level (Table 1). For TIPS-ethynyl-substituted BDCs, the HOMO level elevates in the same order of  $\text{BDF} < \text{TBF} < \text{BDT}$  due to lower ionization potential of the heavier chalcogen atom. Of interest are alkoxy-substituted BDCs with a similar HOMO energy level. It appears that the chalcogen atom effect on the electronic properties of these chromophores somehow depends on the nature of substituents at 4, 8-positions of the BDC core.

TBF derivatives are electron-rich and planar  $\pi$ -systems showing tunable energy levels, intrinsic optical properties, and excellent solubility. Thus, they appear very promising for application in solution-processed organic electronic devices. As a starting point, three well-defined alternating D–A polymers **12a–c** bearing TBF chromophores were synthesized (Scheme 3) and applied in BHJ polymer solar cells. All of them exhibit broad and strong absorptions ranging from 250 to 750 nm, and ambipolar redox properties (Supporting Information) with HOMO levels ranging from −5.34 to −5.15 eV and LUMO levels from −3.44 to −2.78 eV, leading to narrow optical band gaps of 1.66–2.08 eV. As expected, their band gaps as well as their molecular electronic energy levels are readily tuned by copolymerizing the TBF core with different  $\pi$ -conjugated electron-withdrawing units. Bulk heterojunction solar cell devices are fabricated using the photoactive blend layer of the polymer and PCBM ([6,6]-phenyl- $\text{C}_{60}$ -butyric acid methyl ester). A preliminary study has revealed that the devices based on polymer **12a** show power conversion efficiencies (PCE) up to 1.08% under AM 1.5 illumination

(100 mW/cm<sup>2</sup>). Compared to the analogous BDT- and BDF-based polymer solar cells,<sup>21</sup> the first example of TBF-based photovoltaics shows a relatively poor performance, very probably because of their low hole mobilities ( $10^{-5}$ – $10^{-6}$  cm<sup>2</sup> V<sup>−1</sup> s<sup>−1</sup>, see the Supporting Information) and molecular weights. Consequently, in the ongoing study we focus on the systematic modification of the alternating D–A planar copolymer architectures to finely tune absorption coefficients, band gaps, charge mobilities, molecular weights, as well as the blend film morphologies which critically influence the device performance.

In conclusion, we present a polyfunctionalization synthetic strategy to access a family of TBF-based chromophores. Various functional groups are thus introduced to the TBF core allowing late-stage derivatization. Our investigation of the chalcogen-property relationship in these compounds reveals a lowering of the band gap on going from oxygen to sulfur. The nature of substituents at the 4,8-positions of the BDC core plays a crucial role in tuning the electronic properties of the chromophores. As a consequence, the present work gives insight into the structure–property relationship of TBF-type semiconductors and paves a way to develop a manifold of extended  $\pi$ -conjugated TBF molecules and polymers with high structural diversity for high performance device fabrication.

**Acknowledgment.** Financial support for this research by the Swiss National Science Foundation (grant no. 200021-147143) and the Sino Swiss Science and Technology Cooperation is gratefully acknowledged.

**Supporting Information Available.** Experimental procedure and characterization data for all new molecules and polymers, copies of their <sup>1</sup>H NMR spectra, UV–vis spectra of **I**, **3** and **II**, single-crystal structure of **4**, as well as detailed information on device fabrication and characterization. This material is available free of charge via the Internet at <http://pubs.acs.org>.

The authors declare no competing financial interest.

(21) (a) Kim, H. G.; Jo, S. B.; Shim, C.; Lee, J.; Shin, J.; Cho, E. C.; Ihn, S.-G.; Choi, Y. S.; Kim, Y.; Cho, K. *J. Mater. Chem.* **2012**, 22, 17709–17717. (b) Huo, L.; Huang, Y.; Fan, B.; Guo, X.; Jing, Y.; Zhang, M.; Li, Y.; Hou, J. *Chem. Commun.* **2012**, 48, 3318–3320. (c) Chen, X.; Liu, B.; Zou, Y.; Xiao, L.; Guo, X.; He, Y.; Li, Y. *J. Mater. Chem.* **2012**, 22, 17724–17731. (d) Li, H.; Luo, H.; Cao, Z.; Gu, Z.; Shen, P.; Zhao, B.; Chen, H.; Yu, G.; Tan, S. *J. Mater. Chem.* **2012**, 22, 22913–22921.